This is an open access article published under a Creative Commons Attribution (CC-BY) License, which permits unrestricted use, distribution and reproduction in any medium, provided the author and source are cited.

ACS AUTHORCHOICE

THE JOURNAL OF PHYSICAL CHEMISTRY C

pubs.acs.org/JPCC

Article

Time Dependence of Photocurrent in Chemical Vapor Deposition MoS_2 Monolayer—Intrinsic Properties and Environmental Effects

Karolina Czerniak-Łosiewicz,* Arkadiusz P. Gertych, Michał Świniarski, Jarosław Judek, and Mariusz Zdrojek

Cite This: *J. Phys. Chem. C* 2020, 124, 18741−18746

Read Online

ACCESS | Metrics & More | Article Recommendations | Supporting Information

ABSTRACT: We report a model for the description of a room temperature photocurrent temporal response in devices made of a chemical vapor deposition grown molybdenum disulfide monolayer. The proposed model distinguishes three components of a photoresponse that may be attributed to photoconductance and a photogating effect, where photogating involves environmental and intrinsic material contribution. We showed that each time constant obtained from the model differed by an order of magnitude and remained unaffected by changes of the environment, whereas the amplitudes behaved according to the attributed effects. Notably, the rising photocurrent signal was a useful source of information regarding the persistent photoconductivity effect. Finally, we demonstrated the versatility of our model by applying it to some previous reports on time-resolved photocurrent. Our results help to determine the optoelectronic properties of MoS_2 monolayers and future photosensitive devices operating at ambient room temperature.

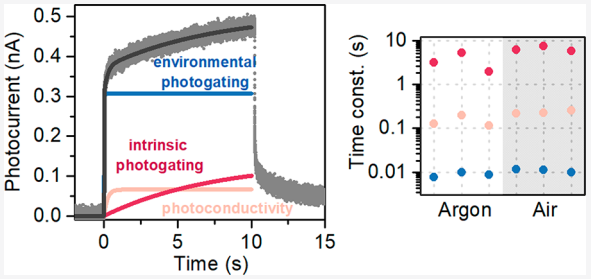

1. INTRODUCTION

Molybdenum disulfide (MoS_2) is a transition metal dichalcogenide (TMD) that exists in a two-dimensional form.[1] Possessing a high on/off current ratio,[2,3] almost negligibly low off-current,[2] and a nonzero, tunable band gap,[4] MoS_2 shows great potential in electronic applications, such as transistors and logic circuits. However, the relatively low mobility of MoS_2 (generally approximately 10 $cm^2\ V^{-1}\ s^{-1}$)[5] may be an issue in modern devices in addition to its sensitivity to ambient conditions.[3] MoS_2 field-effect transistors (FETs) exhibit physisorption of oxygen and water molecules, which reduce on-state current and cause a large hysteresis in transient characteristics.[6] This effect of the ambient environment may be limited with the use of a passivation layer or vacuum measurements.[6−8] Therefore, more attention was brought to the fact that the direct, ∼1.9 eV band gap[1] of MoS_2 monolayers enables current generation under illumination making it a potential candidate for photodetectors and phototransistors operating at low voltage[9] in the visible range of wavelengths.

There are many literature reports about photodetectors based on MoS_2,[9−23] and significant attention was paid to the time dependence of photocurrents in these devices. However, despite the richness of the discussion on this issue, there is no common approach to describe their temporal responses. There are three concepts mainly used for description of time-resolved photocurrent. The first, most widely used description considers the percentage of the obtained signal, especially 90%−10%,[10,16−23] on the rising or decaying side. This method does not include any information about physical phenomena that occur within the material. The second frequently used method including interpretation of the observed phenomenon is the fitting of a stretched exponential function to the decaying part of the photocurrent.[24] The stretching exponent β in this description supposedly reflects the carriers' relaxation mechanism in the material. This method focuses only on relaxation of the photocurrent decay, and it is not widely used to describe the rising photocurrent. The third usual description is fitting a single exponential function[11,12] or sum of two exponentials[13,14,25] and extracting time constants. This description of time−domain photocurrent is informative for physical effects that occur in MoS_2 because these two time constants allow distinguishing between the photoconductive (PC) and photogating (PG) effects to further study these phenomena.[15] The methods of description of the photocurrent are summarized in Table S1 of the Supporting Information.

Most of the mentioned descriptions focus on photocurrent decay after the light was switched off, and the rising photocurrent is generally described by the percentage of the signal. Limited attention was given to the rising signal, which may lead to missing information about the influence of the sample's history on photocurrent and hindering of the possible

Received: May 18, 2020
Revised: August 3, 2020
Published: August 3, 2020

Downloaded via POLITECHNIKA WARSZAWSKA on August 28, 2020 at 06:49:02 (UTC).
See https://pubs.acs.org/sharingguidelines for options on how to legitimately share published articles.

applications. This omission may be due to a common belief that the decaying side of a photocurrent is more likely to reach equilibrium, and therefore, it would be more sensible to extract any time constants from this part. However, studies of persistent photoconductivity (PPC) suggested that this equilibrium state may not be trivial in MoS_2.[14,24] Little to no attention was also given to the physical meaning of the photocurrent description components from the above-mentioned methods. Frequently omitted amplitudes of the exponential fit could also contain important information about photocurrent changes, especially in the continuous operation of a photodetector, where the illumination of the device is repeatedly turned on and off.

In this work we proposed a new approach for the description of time-resolved photocurrent measurements that includes environmental influence on the device. In opposition to the most popular approaches, we fit our model primarily to the rising photocurrent to gain insight into intrinsic photoconductive effect and changes in the photocurrent due to changes in local surface doping[26,27] or persistent photoconductivity effect. Our formula is applicable to both sides of the obtained signal and may be used to compare the results of rise and decay. We distinguished three components in the photoresponse of MoS_2 related to physical phenomena of photoconductive effect, environmental photogating on the surface of MoS_2, and photogating due to intrinsic defects, and we showed the evolution of these effects during environmental changes. Finally, we showed the versatile nature of our model by applying it to the results of different authors to enable a reliable comparison of the results of different samples.

2. EXPERIMENTAL SECTION

The devices were fabricated on a chemical vapor deposition (CVD)-grown MoS_2 sample on sapphire (Sixcarbon Technology, Shenzhen, China) using a standard electron beam lithography technique (Raith e-Line Plus). Sapphire is a dielectric substrate that ensures that the observed photocurrent had no other source than the one originating from MoS_2. Figure 1a shows a Raman spectrum of an as-purchased MoS_2. Raman measurements (Renishaw inVia Raman spectrometer) were taken using a 532 nm line on the prepared device, and the peak position difference between A_{1g} and E_{2g} was 21.3 cm^{-1}, which indicates that the sample was a monolayer.[28,29] Figure 1b presents the photoluminescence spectrum taken with the same spectrometer and 532 nm laser and shows that the tested sample was a monolayer.[4] We also used optical and scanning electron microscopy (SEM) imaging to examine the surface of the prepared devices (see Figure 1c and 1d, respectively). The current response of the device under laser illumination was measured using a homemade setup designed for fast and high-resolution measurements containing a DL 1211 Current Preamplifier and National Instruments DAQ 6366. All results presented in this work were taken applying 5 V source−drain bias. The devices were illuminated with a 532 nm laser with modulated power. They were measured in air and air combined with a direct argon flow. We also performed photocurrent measurements with repeated illumination and the same laser power density. The beam was out of focus to increase the spot size. The mean power densities used were approximately 1.5 W/cm^2 for studying the environmental effect and 170 W/cm^2 for repeated illumination measurements. The data were taken with 10 kHz frequency; each 30 s measurement consists of 300 000 data points in order to capture the rapidly rising photocurrent.

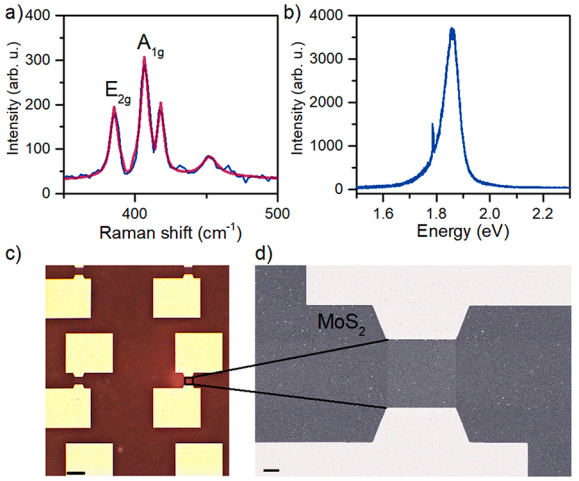

Figure 1. (a) Raman spectrum of MoS_2 on the sapphire substrate with the red line marking a fit of Lorentz functions. (b) Photoluminescence spectrum of the material. (c) Optical image of prepared devices on the sample. Scale bar on the optical image is 100 μm. (d) SEM image of the prepared device. The device is shaped as a 50 μm × 50 μm square. Scale bar on the SEM image is 10 μm.

3. RESULTS AND DISCUSSION

The as-fabricated MoS_2 devices were illuminated (in ambient conditions and in argon flow) to receive a typical response with a rapid increase in the photocurrent and a much slower steady rise which are presented in Figure 2. The illumination was turned off, and we observed another rapid decrease in signal amplitude with a slow decay over time. Changing the sample's environment showed a significant difference in obtained signal as a consequence of different exposure to oxygen molecules. In order to explain this, we proposed a triple-exponential model where the components (see Figure 2) correspond to different physical effects in MoS_2, e.g., environmental changes.

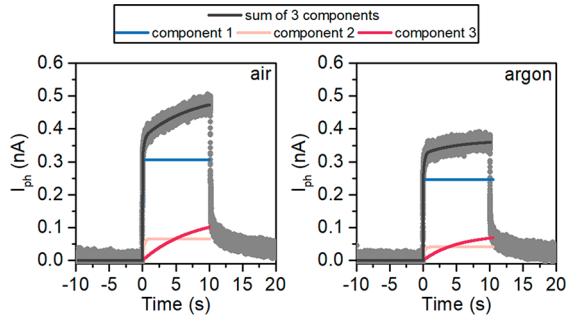

Figure 2. Measured photocurrent in air and in argon flow with fitting of a triple-exponential function. The photocurrent I_{ph} presented here is the difference between the current under illumination and the dark current. The model fits our data perfectly and helps us distinguish three separate components, marked as blue, yellow, and red curves.

We used the model described by the following equation:

$$I(t) = I_{dark} + I_{ph} = I_{dark} + \sum_{k=1}^{3} I_k(1 - e^{-t/\tau_k})$$

https://dx.doi.org/10.1021/acs.jpcc.0c04452
J. Phys. Chem. C 2020, 124, 18741−18746

where τ_k is the time constant, I_k is the amplitude of the fitted function, and I_{dark} is the signal from the sample with no illumination. The novelty of this model is the fitting triple-component $1 - e^{-t/\tau_k}$, which is a solution of a differential equation that is frequently used in physics to describe the effects in a system reaching its equilibrium state; e.g., it describes the change in the concentration of unbalanced photogenerated charge carriers in the time domain.[30] Figure 2 shows that the sum of the three components in our model fits the experimental data perfectly. The extracted time and amplitude components were further marked with corresponding colors: t_1, a_1 as blue; t_2, a_2 as yellow, and t_3, a_3 as red. The fit was performed using boundary conditions, where $t_k > 0$ and $a_k > 0$ on the rising side of the signal (a_k were negative for photocurrent decay). Initial conditions of the fit were t_k = [0.01, 0.1, 1], a_k = [0.1, 1, 10], and the signal was offset by the value of the dark current (fixed $I_{dark} = 0$). The influence of the signal noise on the fit quality was verified to be negligible (see the Supporting Information). Notably, our subsequent analyses focused mainly on the rising side of the photocurrent signal.

To check the influence of air and argon flow, we performed three consecutive measurements in each environment using an incident light power density of approximately 1.5 W/cm^2. Figure 3a shows the time-resolved photocurrent in the atmosphere with prolonged exposure to argon and consecutive measurements in air after the argon flow was removed. Indices 1, 2, and 3 indicate the sequence of measurements, and each measurement was taken for 30 s right after the previous measurement, starting with the measurements in argon. Photocurrent in the air had a higher amplitude, and the plateau was not reached in the time period of measurement. All of the consecutive measurements in argon had similar amplitudes of the signal, but a gradual rise in the amplitude was observed with longer exposure to air. A similar influence of the sample's exposure to oxygen was described previously,[23] and it was explained that, with no illumination, the physiosorbed oxygen was responsible for trapping the electrons in MoS_2, which caused a reduction in the on-state current. When illuminated with sufficient power, the oxygen molecules desorb from the surface,[31] and the photogenerated holes recombine with the trapped electrons. Simultaneously, the photogenerated electrons cause an increase in the measured current. These electrons may be trapped again by oxygen and accumulate in the channel until the irradiation-induced detaching and absorption of the oxygen processes reach equilibrium and cause the plateau in the signal.[23] When the illumination is off, there is an excess of electrons in the system due to prior recombination of the holes. These electrons are trapped again in the channel, which causes a rapid decrease in the photocurrent amplitude. A slow approach to the preillumination current is the result of band-bending near the surface, which hinders electron−hole recombination.[23]

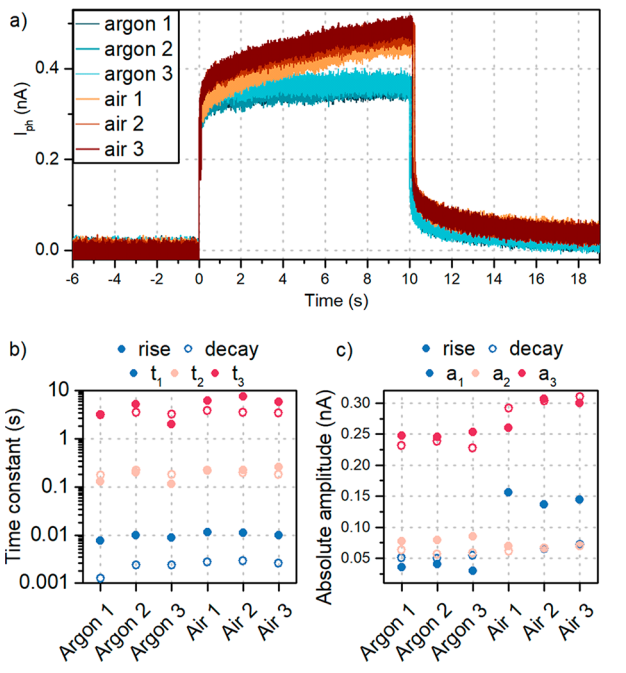

Figure 3. (a) Time-resolved photocurrent measurement of MoS_2 in air and direct argon flow on the sample. The number indicates consecutive measurement in a given atmosphere. The visible increase of the photocurrent in the atmosphere of air is caused by photogenerated electrons while photogenerated holes recombine with electrons trapped by oxygen molecules on the surface of the material. (b) Time constants and (c) amplitudes extracted from the application of the proposed triple-exponential model to our results on rising and decaying sides. Time constants do not show a very significant change in different environments, but two of the three current amplitudes on the rising side of the signal show significant changes.

Application of the proposed model to our measurements data showed three separate components of the photocurrent (Figure 3b and c). We noticed that for the rising photocurrent the response times (t_1, t_2, t_3) differed by an order of magnitude for each separate component but remained almost constant in any given environment. However, the amplitudes (a_1, a_2, a_3) were more similar in values, but there was an obvious change in the a_1 amplitude component (Figure 3c) caused by switching the environment from argon flow to air.

We compared the components from our model on the rising side with components fitted on the decaying signal (Figure 3b and c). For the time constants (Figure 3b), t_2 and t_3 are in good agreement for rise and decay. However, t_1 was decreased by almost an order of magnitude for decay, probably due to the fact that during the measurement the signal does not reach its initial value. For amplitudes (Figure 3c), the situation was similar. Here, a_1 and a_2 were almost constant and equal on the decaying side, but a_3 corresponded to a slight increase of the amplitude, similar to the rising current. The steady amplitude a_1 for the decaying signal may result from laser exposure changes of the surface doping of the sample.[26,31] The separated results for rise and decay are also shown in the Supporting Information. These results show that consideration of only the

https://dx.doi.org/10.1021/acs.jpcc.0c04452
J. Phys. Chem. C 2020, 124, 18741−18746

decaying side of the signal and ignoring the obtained amplitudes of the fit result in missing information about the device's performance, namely, environmentally induced changes. From now on we will focus solely on the rising side of the photocurrent.

We believe that these three components originate from different effects on the sample; namely, the second component (t_2, a_2) is the result of a photoconductive effect, and the first and third components arise from photogating. These two effects were generally distinguished based on the time constants (fast—PC, slow—PG), but our study suggests that we can also extract the constant that is environmentally independent and the one that responds strongly to ambient changes in the PG effect.

The reported PC effect response time ranges from 10 ms[22] to tens of seconds,[14] and it originates from the separation of photoexcited carriers caused by the application of a bias voltage or shallow trap states (band tails resulting from structural defects[15,32]) that trap carriers for a time that is dependent on their depth.[11,14−16,25,33] The PG effect was attributed to two possible causes, which are categorized into external and intrinsic mechanisms. The first source of the PG effect is charge trapping by the surface adsorbates (oxygen and/or water molecules) and the molecules between the substrate and material.[15,16,34] The other source in the off-state are deep midgap recombination centers (associated with the location of the Fermi level), which promote electron−hole recombination.[14−16,25,33] These mechanisms of PG charge trapping were reported with times ranging from over 10 ms[22] up to hundreds of seconds,[14,31] and they are responsible for slow responses of the devices but high values of responsivity.[15,16,22,35]

PG and PC effects were distinguished via the extraction of only two time constants from the temporal photoresponse of MoS_2. We propose a third effect that may also be related to photogating. As shown in Figure 3b and c, in different environments, the time constants stayed almost the same despite the prolonged exposure to argon or air. The environmental change strongly (by approximately four times) affected the a_1 and slightly affected the a_3 amplitude component (by approximately 1.2 times). The t_2 and a_2 constants did not show any changes upon subjection to the ambient environment. Therefore, we attributed the t_2 and a_2 components to the photoconductance and propose distinguishing the photogating effect into environmental photogating and photogating caused by intrinsic material defects using t_1, a_1 and t_3, a_3 components, respectively. The third component may also be related to the saturation of the photocurrent in the samples considering the results shown in Figure 2 (red line corresponding to the shape of a steadily rising current) and Figure 3a, where a slight amplitude increment in the atmosphere of air corresponded to slow and steady growth of the photocurrent until a plateau, unlike in the atmosphere of argon.

To support this hypothesis, we performed 10 consecutive measurements at a higher laser power density than previously (170 W/cm^2) on the same device (Figure 4). These measurements showed three important effects of repeated irradiation of the sample: persistent photoconductivity (PPC), saturation of the photocurrent under laser exposure, and little change in photocurrent decay with the sample's history.

Figure 4a shows the effect of PPC in our measurements. This effect was a lasting conductivity after the light source was

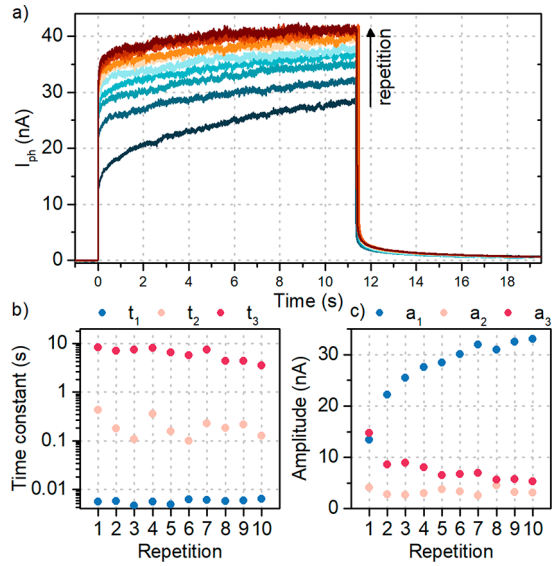

Figure 4. (a) Repeated photocurrent measurements for laser power density of approximately 170 W/cm^2. With each repetition, the photocurrent is closer to reaching its saturation point in a shorter time. The persistent photoconductivity caused an increasingly rapid change in the obtained signal with each repetition. (b) Three time constants almost unaffected by the repetition of measurements. (c) Three amplitudes obtained using our model show a strong influence of the repetition on the a_1 amplitude, a slight decrease in a_3 within the first few repetitions, and a constant a_2 component.

turned off, and it is found in many photoconductive semiconductors, including MoS_2.[14,24,36] This effect is mostly attributed to random localized potential fluctuations in the material that are related to extrinsic sources, especially the substrate (charge traps due to adsorbed water) and defects in the MoS_2 layer, primarily oxygen-related defects.[14,24] With each repeated measurement under illumination, the photocurrent amplitude grew until it reached a saturation point for the last couple of measurements. PPC was more likely to originate from defects in the material rather than in the substrate in our case because the temperature of the CVD process for sample growth should remove any excessive molecules on a bare substrate before the layer is formed. It may also be the reason why the influence of PPC on photocurrent responses resulted in shorter relaxation times in our work compared to the aforementioned studies performed on exfoliated samples.[14] However, our results clearly demonstrated that the rising photocurrent included more information about the sample than the decaying photocurrent. The photocurrent decay values remained similar across the sample's history, at least in the time period around tens of seconds. Therefore, judgment of a device's performance using photocurrent decay alone could result in potentially misleading information about the occurring effects, which may influence potential applications.

Figure 4b and c present the separated components derived using our model. The time constants represent similar behavior to the previously shown results, and they are relatively steady with a slight decrease of the t_3 component (faster saturation). The a_2 amplitude was also constant, which is consistent with our hypothesis that it is related to the PC effect. However, the a_1 amplitude rose logarithmically with each repetition. The logarithmic growth of photocurrent due to PG is related to the increase in the total optical power impinging on a device,[14]

https://dx.doi.org/10.1021/acs.jpcc.0c04452
J. Phys. Chem. C 2020, 124, 18741−18746

which was a PPC-induced effect in our case. These observations further confirm our hypothesis that the three components described the occurring PC and PG effects (second—PC, first—environmental PG, third—intrinsic PG in relation to the saturation of photocurrent).

To examine the versatility of our model, we applied it to a representative selection of literature data,[11,15,18,33,37] which are shown in Figure 5. We found that, despite the differences in the obtained values, we still distinguished three time constants that differed by orders of magnitude (Figure 5a). Figure 5b shows the result of the fitting of our model to the exemplary data from other reports, where we distinguish three components. The differences in the obtained photocurrent signal values are a result of the many factors that contribute to device functioning, such as the quality of the material used, contact resistance, sample's oxidation or age, applied source–drain voltage, or gate voltage. Therefore, the current amplitudes and time constants may differ significantly between the studies. Nevertheless, the evident separation of the time constants demonstrated that the three-component separation of the photocurrent proposed in our model may be used universally and become a tool for comparing the contribution of different effects between authors.

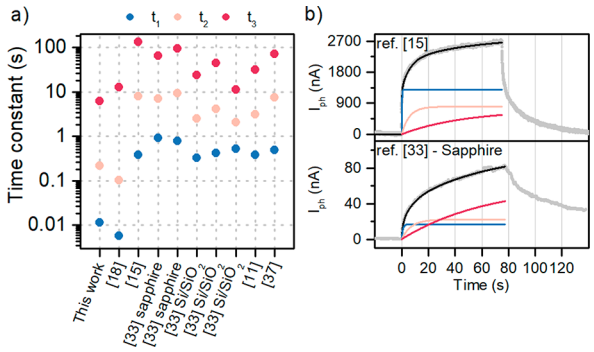

Figure 5. (a) Three components extracted from the fitting of our proposed model to data previously reported in the literature. Despite the variety of the reported photocurrent responses in MoS_2 in different devices, our model distinguishes three time constants that differ by orders of magnitude. (b) Results of the fitting of our model to the data retrieved from works 15 and 33, respectively.

4. CONCLUSIONS

We propose a new versatile model of the photocurrent temporal response of MoS_2-monolayer-based devices with a description that distinguishes three exponential components. Based on the studies of the photocurrent during rapid environmental changes and repeated irradiation, we attributed the second component to photoconductivity, the first component to the environmental photogating effect, and the third component to photogating due to intrinsic mechanisms. To our knowledge, this study is the first time that a photogating effect was distinguished in such a manner. We showed that the rising signal of photocurrents may be a useful carrier of physical information about the sample, especially the sample's history, current saturation, or persistent photoconductivity. We also showed that our model was applicable to experimental data from other authors, which allows for reliable comparisons between reports.

■ ASSOCIATED CONTENT

Supporting Information

The Supporting Information is available free of charge at https://pubs.acs.org/doi/10.1021/acs.jpcc.0c04452.

Summary of the usually used methods of description of the photocurrent in MoS_2; a detailed discussion about the influence of the noise on fit quality; a comparison between fitting results of the rising and decaying sides of the photocurrent signal (PDF)

■ AUTHOR INFORMATION

Corresponding Author

Karolina Czerniak-Łosiewicz − *Faculty of Physics, Warsaw University of Technology, 00-662 Warsaw, Poland;* orcid.org/0000-0002-6781-9374; Phone: +48 22 234 75 46; Email: karolina.czerniak@pw.edu.pl

Authors

Arkadiusz P. Gertych − *Faculty of Physics, Warsaw University of Technology, 00-662 Warsaw, Poland;* orcid.org/0000-0002-7740-9651

Michał Świniarski − *Faculty of Physics, Warsaw University of Technology, 00-662 Warsaw, Poland*

Jarosław Judek − *Faculty of Physics, Warsaw University of Technology, 00-662 Warsaw, Poland*

Mariusz Zdrojek − *Faculty of Physics, Warsaw University of Technology, 00-662 Warsaw, Poland*

Complete contact information is available at: https://pubs.acs.org/10.1021/acs.jpcc.0c04452

Author Contributions

Methodology, investigation, visualization, writing, and original draft preparation (K.C.-Ł.); investigation, writing, review, and editing (A.P.G.); investigation, writing, review, and editing (M.Ś.); conceptualization, methodology, investigation, and supervision (J.J.); writing, review, editing, and supervision (M.Z.).

Notes

The authors declare no competing financial interest.

■ ACKNOWLEDGMENTS

We thank Prof. Thomas Mueller from the Institute of Photonics, Vienna University of Technology and Prof. Ji-Yong Park from the Dept. of Physics and Dept. of Energy Systems Research, Ajou University for sharing their raw data to test the model proposed in this work. This research was supported by the National Center for Research and Development, Poland, within Project No. Lider/180/L-6/14/NCBR/2015 and by TECHMATSTRATEG1/347012/3/NCBR/2017 (HYPERMAT) and partially supported by the CHARMING project (EOS 30467715), funded by the Science Foundation-Flanders (project number G0F6218N).

■ REFERENCES

(1) Mak, K. F.; Lee, C.; Hone, J.; Shan, J.; Heinz, T. F. Atomically Thin MoS 2: A New Direct-Gap Semiconductor. *Phys. Rev. Lett.* **2010**, *105*, 136805.

(2) Radisavljevic, B.; Radenovic, A.; Brivio, J.; Giacometti, V.; Kis, A. Single-Layer MoS2 Transistors. *Nat. Nanotechnol.* **2011**, *6* (3), 147–150.

(3) Qiu, H.; Pan, L.; Yao, Z.; Li, J.; Shi, Y.; Wang, X. Electrical Characterization of Back-Gated Bi-Layer MoS 2 Field-Effect

Transistors and the Effect of Ambient on Their Performances. *Appl. Phys. Lett.* **2012**, *100* (12), 123104.
(4) Splendiani, A.; Sun, L.; Zhang, Y.; Li, T.; Kim, J.; Chim, C. Y.; Galli, G.; Wang, F. Emerging Photoluminescence in Monolayer MoS2. *Nano Lett.* **2010**, *10* (4), 1271−1275.
(5) Novoselov, K. S.; Jiang, D.; Schedin, F.; Booth, T. J.; Khotkevich, V. V.; Morozov, S. V.; Geim, A. K. Two-Dimensional Atomic Crystals. *Proc. Natl. Acad. Sci. U. S. A.* **2005**, *102* (30), 10451−10453.
(6) Late, D. J.; Liu, B.; Matte, H. S. S. R.; Dravid, V. P.; Rao, C. N. R. Hysteresis in Single-Layer MoS 2 Field Effect Transistors. *ACS Nano* **2012**, *6* (6), 5635−5641.
(7) Qiu, H.; Pan, L.; Yao, Z.; Li, J.; Shi, Y.; Wang, X. Electrical Characterization of Back-Gated Bi-Layer MoS 2 Field-Effect Transistors and the Effect of Ambient on Their Performances. *Appl. Phys. Lett.* **2012**, *100* (12), 123104.
(8) Ahn, J. H.; Parkin, W. M.; Naylor, C. H.; Johnson, A. T. C.; Drndić, M. Ambient Effects on Electrical Characteristics of CVD-Grown Monolayer MoS2 Field-Effect Transistors. *Sci. Rep.* **2017**, *7* (1), 1−9.
(9) Perea-López, N.; Lin, Z.; Pradhan, N. R.; Iñiguez-Rábago, A.; Elías, A. L.; McCreary, A.; Lou, J.; Ajayan, P. M.; Terrones, H.; Balicas, L. CVD-Grown Monolayered MoS2 as an Effective Photosensor Operating at Low-Voltage. *2D Mater.* **2014**, *1* (1), 011004.
(10) Li, X.; Wu, J.; Mao, N.; Zhang, J.; Lei, Z.; Liu, Z.; Xu, H. A Self-Powered Graphene-MoS2 Hybrid Phototransistor with Fast Response Rate and High on-off Ratio. *Carbon* **2015**, *92*, 126−132.
(11) Lopez-Sanchez, O.; Lembke, D.; Kayci, M.; Radenovic, A.; Kis, A. Ultrasensitive Photodetectors Based on Monolayer MoS 2. *Nat. Nanotechnol.* **2013**, *8* (7), 497−501.
(12) Khan, M. F.; Nazir, G.; Lermolenko, V. M.; Eom, J. Electrical and Photo-Electrical Properties of MoS2 Nanosheets with and without an Al2O3 Capping Layer under Various Environmental Conditions. *Sci. Technol. Adv. Mater.* **2016**, *17* (1), 166−176.
(13) Han, P.; St. Marie, L.; Wang, Q. X.; Quirk, N.; El Fatimy, A.; Ishigami, M.; Barbara, P. Highly Sensitive MoS2 Photodetectors with Graphene Contacts. *Nanotechnology* **2018**, *29* (20), 20LT01.
(14) Di Bartolomeo, A.; Genovese, L.; Foller, T.; Giubileo, F.; Luongo, G.; Croin, L.; Liang, S. J.; Ang, L. K.; Schleberger, M. Electrical Transport and Persistent Photoconductivity in Monolayer MoS2 Phototransistors. *Nanotechnology* **2017**, *28* (21), 214002.
(15) Furchi, M. M.; Polyushkin, D. K.; Pospischil, A.; Mueller, T. Mechanisms of Photoconductivity in Atomically Thin MoS2. *Nano Lett.* **2014**, *14* (11), 6165−6170.
(16) Kufer, D.; Konstantatos, G. Highly Sensitive, Encapsulated MoS2 Photodetector with Gate Controllable Gain and Speed. *Nano Lett.* **2015**, *15* (11), 7307−7313.
(17) Tang, W.; Liu, C.; Wang, L.; Chen, X.; Luo, M.; Guo, W.; Wang, S. W.; Lu, W. MoS2 Nanosheet Photodetectors with Ultrafast Response. *Appl. Phys. Lett.* **2017**, *111* (15), 153502.
(18) Moun, M.; Singh, A.; Tak, B. R.; Singh, R. Study of the Photoresponse Behavior of a High Barrier Pd/MoS2/Pd Photodetector. *J. Phys. D: Appl. Phys.* **2019**, *52* (32), 325102.
(19) Lee, H. S.; Min, S. W.; Chang, Y. G.; Park, M. K.; Nam, T.; Kim, H.; Kim, J. H.; Ryu, S.; Im, S. MoS2 Nanosheet Phototransistors with Thickness-Modulated Optical Energy Gap. *Nano Lett.* **2012**, *12* (7), 3695−3700.
(20) Kaushik, V.; Varandani, D.; Das, P.; Mehta, B. R. Layer Dependent Photoresponse Behavior of Chemical Vapor Deposition Synthesized MoS2 Films for Broadband Optical Sensing. *J. Phys. D: Appl. Phys.* **2019**, *52* (47), 475302.
(21) Tsai, D. S.; Liu, K. K.; Lien, D. H.; Tsai, M. L.; Kang, C. F.; Lin, C. A.; Li, L. J.; He, J. H. Few-Layer MoS2 with High Broadband Photogain and Fast Optical Switching for Use in Harsh Environments. *ACS Nano* **2013**, *7* (5), 3905−3911.
(22) Gant, P.; Huang, P.; Pérez de Lara, D.; Guo, D.; Frisenda, R.; Castellanos-Gomez, A. A Strain Tunable Single-Layer MoS2 Photodetector. *Mater. Today* **2019**, *27*, 8−13.
(23) Pak, J.; Min, M.; Cho, K.; Lien, D. H.; Ahn, G. H.; Jang, J.; Yoo, D.; Chung, S.; Javey, A.; Lee, T. Improved Photoswitching Response Times of MoS2 Field-Effect Transistors by Stacking p -Type Copper Phthalocyanine Layer. *Appl. Phys. Lett.* **2016**, *109* (18), 183502−5.
(24) Wu, Y. C.; Liu, C. H.; Chen, S. Y.; Shih, F. Y.; Ho, P. H.; Chen, C. W.; Liang, C. Te; Wang, W. H. Extrinsic Origin of Persistent Photoconductivity in Monolayer MoS2 Field Effect Transistors. *Sci. Rep.* **2015**, *5* (June), 1−10.
(25) Di Bartolomeo, A.; Grillo, A.; Urban, F.; Iemmo, L.; Giubileo, F.; Luongo, G.; Amato, G.; Croin, L.; Sun, L.; Liang, S. J.; et al. Asymmetric Schottky Contacts in Bilayer MoS2 Field Effect Transistors. *Adv. Funct. Mater.* **2018**, *28* (28), 1800657.
(26) Rao, R.; Carozo, V.; Wang, Y.; Islam, A. E.; Perea-Lopez, N.; Fujisawa, K.; Crespi, V. H.; Terrones, M.; Maruyama, B. Dynamics of Cleaning, Passivating and Doping Monolayer MoS2 by Controlled Laser Irradiation. *2D Mater.* **2019**, *6* (4), 045031.
(27) Oh, H. M.; Han, G. H.; Kim, H.; Bae, J. J.; Jeong, M. S.; Lee, Y. H. Photochemical Reaction in Monolayer MoS2 via Correlated Photoluminescence, Raman Spectroscopy, and Atomic Force Microscopy. *ACS Nano* **2016**, *10* (5), 5230−5236.
(28) Lee, C.; Yan, H.; Brus, L. E.; Heinz, T. F.; Hone, J.; Ryu, S. Anomalous Lattice Vibrations of Single- and Few-Layer MoS2. *ACS Nano* **2010**, *4* (5), 2695−2700.
(29) Li, H.; Zhang, Q.; Yap, C. C. R.; Tay, B. K.; Edwin, T. H. T.; Olivier, A.; Baillargeat, D. From Bulk to Monolayer MoS 2: Evolution of Raman Scattering. *Adv. Funct. Mater.* **2012**, *22* (7), 1385−1390.
(30) Shalimova, K. V. *Physics of Semiconductors*; Wydawnictwo Naukowe PWN: Moscow, 1974.
(31) Han, P.; Adler, E. R.; Liu, Y.; St Marie, L.; El Fatimy, A.; Melis, S.; Van Keuren, E.; Barbara, P. Ambient Effects on Photogating in MoS2 Photodetectors. *Nanotechnology* **2019**, *30* (28), 284004.
(32) Ghatak, S.; Ghosh, A. Observation of Trap-Assisted Space Charge Limited Conductivity in Short Channel MoS2 Transistor. *Appl. Phys. Lett.* **2013**, *103* (12), 122103.
(33) Nguyen, V. T.; Ha, S.; Yeom, D. Il; Ahn, Y. H.; Lee, S.; Park, J. Y. Large-Scale Chemical Vapor Deposition Growth of Highly Crystalline MoS2 Thin Films on Various Substrates and Their Optoelectronic Properties. *Curr. Appl. Phys.* **2019**, *19* (10), 1127−1131.
(34) Miller, B.; Parzinger, E.; Vernickel, A.; Holleitner, A. W.; Wurstbauer, U. Photogating of Mono- and Few-Layer MoS2. *Appl. Phys. Lett.* **2015**, *106* (12), 122103.
(35) Buscema, M.; Island, J. O.; Groenendijk, D. J.; Blanter, S. I.; Steele, G. A.; Van Der Zant, H. S. J.; Castellanos-Gomez, A. Photocurrent Generation with Two-Dimensional van Der Waals Semiconductors. *Chem. Soc. Rev.* **2015**, *44* (11), 3691−3718.
(36) Zhang, W.; Huang, J. K.; Chen, C. H.; Chang, Y. H.; Cheng, Y. J.; Li, L. J. High-Gain Phototransistors Based on a CVD MoS2Monolayer. *Adv. Mater.* **2013**, *25* (25), 3456−3461.
(37) Zhou, Y. H.; An, H. N.; Gao, C.; Zheng, Z. Q.; Wang, B. UV-Vis-NIR Photodetector Based on Monolayer MoS2. *Mater. Lett.* **2019**, *237*, 298−302.

https://dx.doi.org/10.1021/acs.jpcc.0c04452
J. Phys. Chem. C 2020, 124, 18741−18746